# HARE: Hybrid ARQ-Based Adaptive Retransmission Control Scheme for Synchronous Multi-Link in Wireless LANs

Taewon Song and Woong-Hee Lee

***Abstract*—As the resolution of video becomes high and the number of mobile devices proliferates, the demand for video traffic is exploding. New traffic types, such as augmented reality (AR) and virtual reality (VR), which require high-throughput and low-latency, are also emerging. Two of the promising techniques discussed in increasing throughput and lowering latency are multi-link transmission and hybrid automatic repeat request (HARQ). However, in most cases of a device using a low-cost chipset, there are potential limitations to using HARQ on multi-link. This article proposes a HARQ-based adaptive retransmission control scheme (HARE), which determines the optimal retransmission policy by casting it as a Markov decision process (MDP) for the devices undergoing the aforementioned limitations. Through this, we can decide whether to execute HARQ and select the adequate modulation and coding rate when a retransmission occurs. Through extensive analysis, we found that HARE can greatly increase throughput compared to the ARQ-only and HARQ-only retransmission methods with a small amount of buffer occupancy. This technique expects high-resolution video and brand-new services such as AR/VR to be enjoyed even by the devices with low-cost chipsets.**

***Index Terms*—IEEE 802.11be, hybrid ARQ, Markov decision process, multi-link operation, Wi-Fi 7.**

## I. Introduction

WIRELESS local area network (WLAN) plays an increasingly important role in providing wireless data services in various environments, such as homes and businesses. In particular, video traffic is becoming the dominant traffic type for WLAN traffic, and the throughput requirement for this video traffic continues to increase with the advent of 4 k and 8 k video [1]. Additionally, throughput requirements from low-latency applications and new applications such as augmented and virtual reality (AR/VR), gaming, remote offices, and cloud computing will also increase. Along with the natural increase in throughput demands with advances in these technologies, staying home over the COVID-19 concerns brings about more demands on the throughput of video traffic [2].

IEEE 802.11, the de facto standard for WLANs, has been amended over decades to provide wireless stations with improved data rates. These amendments employ multi-user multiple input multiple output (MU-MIMO), high-density modulation, and wider channel bandwidth to increase supported physical data rates. They can also improve frequency efficiency through orthogonal frequency division multiple access (OFDMA) and spatial reuse based on improved computing power. In 2019, IEEE 802.11 began discussing a new revision called IEEE 802.11be-Extreme High Throughput (EHT) [3], which will be called Wi-Fi 7, where end users can expect more increased throughput, improved reliability, reduced delay and jitter, and enhanced power efficiency within WLAN applications. In order to accelerate the standard development process, the standardization group has agreed to select a small feature set (Release 1) of high priorities to be released by 2021. Release 1 includes 320 MHz bandwidth, 4K-quadrature amplitude modulation (QAM), and multi-link support, which can provide high performance gain with low complexity. Release 2, on the other hand, included relatively complex features such as hybrid automatic repeat request (HARQ), 16 spatial streams, and multiple access point (multi-AP) features.

HARQ [4], [5], [6] is one of the candidate features which is beneficial to increasing data rate and reducing transmission delay. The HARQ has been widely used in various communication systems, such as universal mobile telecommunications system (UMTS), mobile WiMAX, and long-term evolution (LTE) wireless networks. Unlike legacy retransmission procedures in conventional IEEE 802.11, HARQ enables soft-combining or additional parity at the receiver to improve the probability of correct decoding. As a result, the receiver can increase the actual signal-to-noise ratio (SNR) by storing the erroneously decoded packet and combining it with subsequent retransmissions before decoding with HARQ.

In the above-mentioned communication protocol, since the introduction of HARQ has matured, a number of advanced

Manuscript received 1 June 2022; revised 2 December 2022 and 17 January 2023; accepted 6 March 2023. Date of publication 15 March 2023; date of current version 15 August 2023. This work was supported in part by Electronics and Telecommunications Research Institute funded by ICT R&D Program of MSIT/IITP under Grant 2021-0-00746, Development of Tbps wireless communication technology, in part by the National Research Foundation of Korea funded by the Korea Government, MSIT under Grant 2022R1F1A1076069, and in part by Regional Innovation Strategy through the National Research Foundation of Korea (NRF) funded by the Ministry of Education under Grant 2021RIS-004. The review of this article was coordinated by Dr. Zehui Xiong. *(Corresponding author: Woong-Hee Lee.)*

Taewon Song is with the Department of Internet of Things, SCH MediaLabs, Soonchunhyang University, Asan-si, Chungcheongnam-do 31538, Korea (e-mail: twsong@sch.ac.kr).

Woong-Hee Lee is with the Department of Control and Instrumentation Engineering, Korea University, Sejong-si 30019, Republic of Korea (e-mail: woongheelee@korea.ac.kr).

Digital Object Identifier 10.1109/TVT.2023.3257424

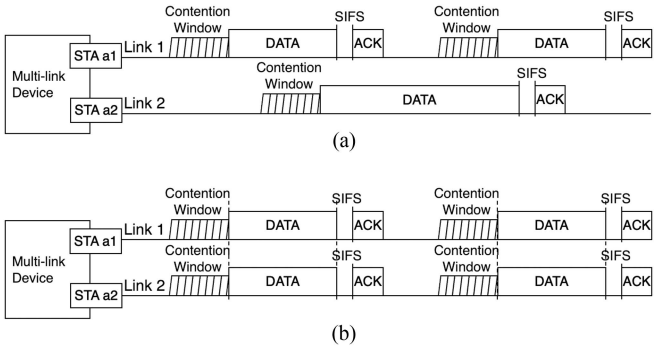


Fig. 1. (a) Asynchronous, (b) Synchronous transmission examples in multi-link environment.

techniques have also been proposed. Adaptive HARQ [7] has been proposed to achieve ultra-reliable communication with low delay. The methodology of adaptive HARQ and our proposed method, HARE, are somewhat similar to adaptively determining retransmission in HARQ. The difference between our proposed method and the existing adaptive HARQ is that the numerology is different due to the different communication protocol standard. Furthermore, multiple links are not assumed in the conventional adaptive HARQ.

Specifically, three popular HARQ methods have been discussed in IEEE 802.11be: chase combining (CC) where every retry will contain the same information as the initial transmission [8], [9], punctured CC (PCC) where the transmitter repeats only a fraction of the coded bits with low SNR [10], [11], [12], and incremental redundancy (IR) where every retransmission uses a different set of coded bits representing the same set of information bits [12], [13], [14], [15]. Among these three methods, CC is the most appropriate method for entry-level multi-link devices because it can be easily performed with low complexity. Although IR is the most difficult to implement, it is the most efficient in terms of SNR gain. PCC provides moderate performance compared to CC and IR.

Meanwhile, not all the multi-link devices can fulfill the benefits of adopting HARQ on the multi-link operation. For example, devices with low-cost entry-level chipsets are likely to have poor in-device interference cancellation performance. Therefore, they have no choice but to transmit and receive frames in an aligned manner due to the in-device interference. Meanwhile, due to computational limitations for the devices, they may only have to use HARQ-CC.

Another approach under discussion in IEEE 802.11be that meets the throughput and strict delay limits is native support for the multi-link operation, allowing multiple bands or links to be used simultaneously with multiple radio interfaces attached to one device. Particularly, there are two types of multi-link transmissions, as illustrated in Fig. 1, according to the capability of simultaneous transmissions on multiple links, namely, asynchronous multi-link [16] and synchronous multi-link transmissions [16], [17], [18], [19], [20], [21], [22]. The asynchronous transmission inherits the conventional channel access mechanism in the conventional IEEE 802.11. In contrast, the synchronous transmission is the modified one to support constrained stations, which cannot support simultaneous transmission and reception. For the asynchronous multi-link transmission, as shown in Fig. 1(a), a device behaves as if it has multiple independent stations without any interference between the links, and therefore can transmit and receive at any moment. On the other hand, for the synchronized multi-link transmission, as shown in Fig. 1(b), a device shall transmit or receive frames on multiple links with alignment of transmission starting and ending time to avoid interference. This alignment is inevitable when the frequency isolation between the center frequencies of the links is not far enough, or an in-device interference cancellation is not sufficient due to lack of ability for a device to attenuate internal radio signals.

There are numerous researches based on IEEE 802.11be multi-link environments. There have been lots of studies to reveal efficiency to use synchronous multiple links. The impacts of request-to-send (RTS)/clear-to-send (CTS) exchange, the number of stations, the length of data units, and various parameters on network throughput have been investigated [23]. In [24], the authors considered how to allocate flows to which links when new traffic flows occur. However, the study was focusing on traffic allocation policy and it lacks considerations on asynchronous and synchronous transmissions on multi-link. To overcome synchronous multi-link transmission, the authors proposed a newly designed channel access scheme to maximize the utilization of wireless medium for devices with limited interference cancellation for a station that does not have the ability to simultaneously receive on one channel while transmitting on another channel in [25]. Also in [26], the authors expanded above discussion for mobile access points (APs) that cannot transmit and receive simultaneously. With transmission alignment with ongoing transmission on the other link, they showed that the lack of simultaneous transmit and receive capability can be compensated. Also, it is found that the concurrent usage of multiple radio interfaces may introduce new obstacles [27]. Although the mentioned studies were dealing with and overcoming the synchronous transmission problem, they do not consider the HARQ technique that can improve the throughput.

HARQ is a method that can directly improve throughput. IR can provide higher throughput compared to CC, but it is not applicable to all chipsets because it requires additional implementation and internal speed requirements within the chipset, so it is expected that CC will be applied to many entry-level chipsets. In addition, in the case of a low-end chipset, as mentioned above, it seems that synchronization between transmitted data units must be performed due to the in-device interference problem. This is a problem that low-end chipsets will face when 802.11be is introduced, so it needs to be addressed and is the main scope of this study.

In this article, we propose HARQ-based Adaptive REtransmission control scheme (HARE), where a transmitter (i.e., a non-access point multi-link device) transmits frames to a receiver (i.e., an access point multi-link device), and each device has two radio interfaces. The transmitter decides whether to use HARQ and which modulation and coding scheme (MCS) to use to maximize expected throughput while maintaining an

appropriate level of buffered data on the receiver side, under the premise of HARQ-CC based on the synchronized multi-link operation. To this end, we formulate an analytical model based on a Markov decision process (MDP) and obtain an optimal policy maximizing delivered information while reducing buffer occupancy by value iteration, which is one of representative approaches to derive an optimal policy in MDP using Bellman optimality equation. Performance analysis results show that HARE can improve expected throughput with a small buffer occupancy.

The contributions of this article are twofolds:

- To the best of our knowledge, this is the first work to decide optimal policy considering multiple radio interfaces, operating based on synchronous multi-link transmission.
- We jointly consider buffer status on receiver side and channel coherence time to decide optimal policy for HARQ-CC.

The remainder of this article is organized as follows. The system model and protocol description of HARE are presented in Section II. The formulation of MDP of HARE is described in Section III. Performance evaluation results and conclusion are given in Sections IV and V, respectively.

## II. Hybrid ARQ Based Adaptive Retransmission Control Scheme

In this section, we first introduce the system model for HARE and then explain its operational protocol in more detail.

### A. System Description

In IEEE 802.11be, a new logical entity named multi-link device (MLD) is defined. MLD has more than one affiliated stations and has a single medium access control service access point to logical link control, which includes one MAC data service. AP MLD and non-AP MLD are MLDs in which each station affiliated with the MLD is an AP and a station, respectively.

In this literature, we assume the MLD consists of two stations that operate in different bands. Although these stations affiliated with a single non-AP MLD may be associated with different APs, we assume that a non-AP MLD is being associated with an AP MLD having the same structure. We consider a non-AP MLD that wishes to transmit data frames to the associating AP MLD. Each AP has a buffer that can combine erroneous data frames with previous data frames through the HARQ process.

When it comes to HARQ operation, HARQ-CC is considered. In other words, a transmitter will retransmit the data frame containing the same information with the same modulation and code rate as the previous transmission. HARQ granularity follows the physical-layer protocol data unit (PPDU) level. Hence, an entire PPDU will be combined with the subsequent PPDU for HARQ combining. We also assume that stations affiliated with the same MLD can only transmit or receive at the same time. A MAC sublayer for conventional IEEE 802.11 WLAN is divided into MLD lower MAC sublayer and MLD upper MAC sublayer. The MLD upper MAC sublayer functions include authentication, association, security association, and MLD level management. The MLD lower MAC sublayer functions include link-specific control information exchange/indication. The block ack score boarding function is performed through cooperation between upper and lower layers. A structure of AP MLD and non-AP MLD adopted in this literature is illustrated in Fig. 2.

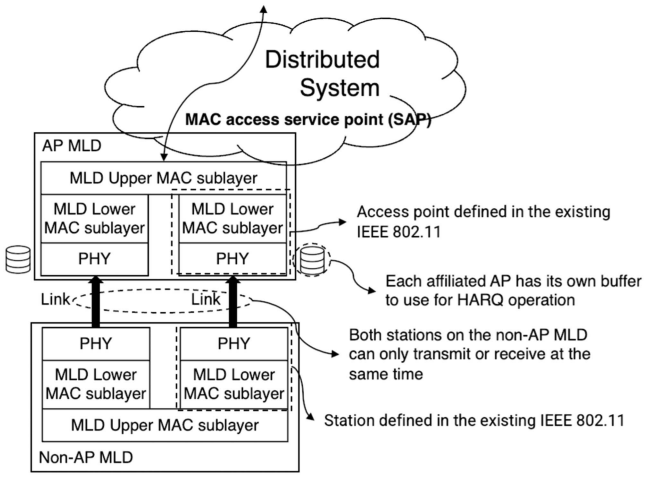


Fig. 2. High level architecture for AP MLD and the non-AP MLD with two stations, respectively.

### B. Protocol Description

In this subsection, we describe an uplink transmission and reception procedure for non-AP MLD and AP MLD, as shown in Fig. 3.

When a transmitter, a non-AP MLD in this literature, wishes to transmit frames, the transmitter first collects state information to decide its action. The collected state information consists of the number of buffered frames to be combined, the previous MCS, the transmission result of the previous transmission, the channel condition, and the number of available slots of the channel coherence time. The action consists of 1) whether to use HARQ and 2) which MCS to use for the transmission using a value iteration algorithm based on the collected state information. The transmitter may indicate the selected action on the PHY header. If the corresponding transmission is not the initial transmission and the transmitter decides to use HARQ, the MCS for the retransmission must be the same as the previous transmission to combine the signals to get an SNR gain. Furthermore, since we consider the synchronous transmission, the MCSs among the transmissions on the multiple links should also be the same. The action determination procedure takes place in the gray boxes. After deciding the non-AP MLD's action through HARE, the non-AP MLD transmits data frames through multiple radio interfaces and waits for the receiver's corresponding responses.

After that, a receiver, an AP MLD in this literature, will receive data frames through multiple links. The receiver can figure out whether the transmitter applies HARQ or not. If the HARQ is applied and there are buffered frames to be combined, the receiver combines the received frames with the buffered frames and decodes them. When the receiver detects that the HARQ is disabled, the receiver decodes the received frames without buffered frames in the same way as previously defined in conventional 802.11. According to the decoding result, the

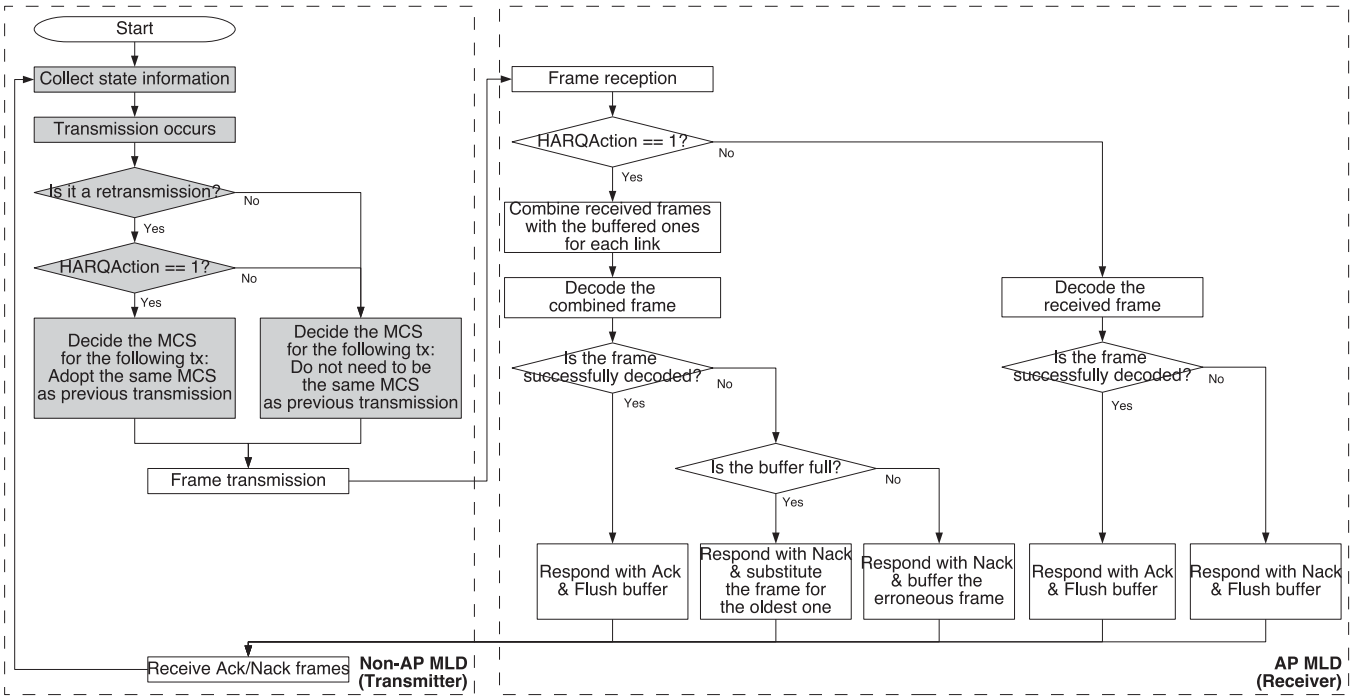


Fig. 3. Block diagram of HARQ based adaptive retransmission control scheme.

receiver responds to the transmitter with the acknowledgement (Ack) or the negative acknowledgement (Nack) frame. One remarkable thing is that only when the HARQ is applied and the frame is not successfully decoded, the receiver buffers it to combine for the next retransmission. Otherwise, the receiver flushes out the buffer for the corresponding frame.

Getting back to the transmitter side, we can see that the transmitter renews its state information by the received acknowledgment frames and tries the next transmission with the renewed state information.

## III. MDP Formulation of HARE

The MDP model is an appropriate mathematical framework for decision making. In this section, we present an MDP model for uplink retransmission control operation and derive an optimal policy for determining whether to use HARQ and an MCS to be used. Used notations for the MDP model are listed in Table I.

### A. Decision Epoch

Each decision occurs when a transmitter tries to transmit a data frame. In this article, it is assumed that the frame exchange sequence's duration, that is to say, the transmission time during the data frame and the subsequent Ack frame, is fixed at $T_p$. Specifically, the stations affiliated with the non-AP MLD transmit data frames and then receive corresponding acknowledgment frames in a duration of $T_p$. Since an MDP model requires the state space to be finite, we consider the block fading channel model [28], [29], [30], where the channel is assumed to be fixed for the channel coherence time, $T_c$. The channel coherence time can be

TABLE I
Summary of Notations

| Notation | Description |
|---|---|
| $\mathbf{S}$ | State space |
| $\mathbf{B}$ | Buffer state |
| $\mathbf{M}_S$ | MCS state for the state space |
| $\mathbf{K}$ | Acknowledgment state |
| $\mathbf{C}$ | Channel state |
| $\mathbf{F}$ | Available slot state |
| $\mathbf{A}$ | Action set |
| $\mathbf{H}$ | HARQ action set |
| $\mathbf{M}_A$ | MCS state for the action set |
| I | Link set |
| $B_{\max}$ | Number of capable buffer size maximum retransmission count for HARQ |
| $M$ | The largest supportable MCS |
| $c_{\max}$ | Number of discretized channels |
| $F_{\max}$ | Maximum number of slots for channel coherence |

calculated according to the velocity of a device as follows [31]:

$$T_c = \sqrt{\frac{9}{16\pi}}\frac{1}{f_m}, \tag{1}$$

where $f_m$ is the maximum Doppler shift, given by $f_m = (v/c) \cdot f_c$ with $f_c$ being the center frequency of the transmitting device, with $v$ being the velocity of the transmitting device, and with $c$ the speed of light. In conclusion, the device can make at most $F_{\max} = \lceil T_c/T_p \rceil$ attempts without time-varying channel conditions.

### B. State Space

We define the state space of a finite set $\mathbf{S}$ as follows:

$$\mathbf{S} = \mathbf{B} \times \mathbf{M}_S \times \mathbf{K} \times \mathbf{C} \times \mathbf{F}, \tag{2}$$

where $\mathbf{B}$, $\mathbf{M}_S$, $\mathbf{K}$, $\mathbf{C}$, and $\mathbf{F}$ are as expressed in Table I.

First, for $\mathbf{B}$, the transmitter needs to infer the receiver's buffer information. This can be easily done by receiving an Ack or Nack frame from the receiver. $\mathbf{B}$ can be defined as a Cartesian product of the sets of each AP's buffer as follows:

$$\mathbf{B} = \prod_{i \in I} \mathbf{B}_i, \tag{3}$$

where $\mathbf{B}_i$ denotes the set of available buffer amounts for the receiver on the link $i$. Expressing the maximum amount of buffer per one frame allowed as $B_{\max}$, we can define $\mathbf{B}_i$ as $\mathbf{B}_i = \{0, 1, \ldots, B_{\max}\}$. $B_{\max}$ can also be considered as the maximum number of HARQ retransmissions. For example, when there are two links and they can only buffer one space per a frame, $\mathbf{B}$ can be defined as $\mathbf{B} = \{(0,0), (0,1), (1,0), (1,1)\}$.

$\mathbf{M}_S$, indicating the previous transmission's MCS values, is represented by

$$\mathbf{M}_S = \{1, 2, \ldots, M\}, \tag{4}$$

where $M$ is the largest MCS value supported. For $\mathbf{M}_S$, supportable MCS can be expressed by numbering in ascending order.

$\mathbf{K}$ can be expressed in a similar way to $\mathbf{B}$. By receiving the responses from the transmitter, the receiver can notice whether the previous data transmissions are successfully received or not. $\mathbf{K}$ is represented by

$$\mathbf{K} = \prod_{i \in I} \mathbf{K}_i, \tag{5}$$

where $\mathbf{K}_i$ indicates the Ack or the Nack on the link $i$. $\mathbf{K}_i$ can be represented by $\mathbf{K}_i = \{0, 1\}$, where 0 and 1 stand for the Nack and the Ack, respectively.

$\mathbf{C}$ is the set of discrete channel states discretized into $C_{\max}$ levels under the channel model explained in Section III-A. As we are considering multiple link environment, $\mathbf{C}$ can be expressed as

$$\mathbf{C} = \prod_{i \in I} \mathbf{C}_i, \tag{6}$$

where $\mathbf{C}_i$ stands for the discretized channel status on the link $i$, which is, $\mathbf{C}_i = \{1, 2, \ldots, C_{\max}\}$, with numbering them in ascending order. Our discrete channel model is based on the classical two-state Gilbert–Elliott model [32], [33] with finite-state Markov channel (FSMC) for rayleigh fading channels [34].

Finally, $\mathbf{F}$ describes the set of number of available slots until the channel coherence ends. $\mathbf{F}$ can be expressed as

$$\mathbf{F} = \{0, 1, \ldots, F_{\max} - 1\}, \tag{7}$$

as mentioned in Section III-A.

Along with the definitions mentioned above, we further define another state space of a finite set $\mathbf{S}_i$ for a particular link $i$ as

$$\mathbf{S}_i = \mathbf{B}_i \times \mathbf{M}_S \times \mathbf{K}_i \times \mathbf{C}_i \times \mathbf{F}. \tag{8}$$

### C. Action Space

Based on the state information in Section III-B, the transmitter picks out an action $a$ that consists of whether to use HARQ and which MCS to transmit based on MDP model. To do this, we define the action state as follows:

$$\mathbf{A} = \mathbf{H} \times \mathbf{M}_A. \tag{9}$$

$\mathbf{H}$ represents whether to use HARQ. Hence, $\mathbf{H}$ can simply be expressed as $\mathbf{H} = \{0, 1\}$. If the transmitter wants to apply HARQ for the next (re)transmission, it will take the value of 1. Otherwise, it will take the value of 0. A specific procedure will be stated as follows.

- HARQ: If the HARQ action is taken, the receiver receives and decodes the data frame with the buffered data if any. If the buffer is empty, the receiver decodes the frame as is. In other words, the transmitter can enable HARQ action regardless of whether the transmission is an initial transmission or a retransmission. When the data frame is successfully decoded, the buffer will be flushed out. Otherwise, the receiver stacks up the current data frame on top of its buffer until the buffer is full.
- No HARQ: Suppose the transmitter decides not to take the HARQ action, and the receiver becomes aware of it. In that case, the receiver first flushes out the buffer regardless of the previous transmission's acknowledgment. Also, no matter whether the decoding of the current reception was successful or not, the receiver does not buffer the data frame.

Next, the transmitter can also pick out the MCS value among the supportable MCSs, which is identical to (4). $\mathbf{M}_A$ can be expressed as

$$\mathbf{M}_A = \{1, 2, \ldots, M\}. \tag{10}$$

In addition, The sets of MCSs for the state space $\mathbf{M}_S$ and that of the action space $\mathbf{M}_A$ can be distinguished by subscript.

### D. State Transition Function

We denote two arbitrary states in $\mathbf{S}$ as $s = \{b, m_S, k, c, f\}$ and $s' = \{b,' m_S,' k,' c,' f'\}$, and an arbitrary action in $\mathbf{A}$ as $a = \{h, m_A\}$. Since each of $b$, $k$, and $c$ has $N$ elements, we denote the elements of them with the subscription. For example, the number of buffers, the Ack state, and the channel state for the station affiliated with an MLD on the link $i$ are $b_i$, $k_i$, and $c_i$, respectively. Then, we can also define two arbitrary states for a particular link $i$ in $\mathbf{S}_i$ as $s_i = \{b_i, m_S, k_i, c_i, f\}$ and $s_i' = \{b_i,' m_S,' k_i,' c_i,' f'\}$.

The state transition function is the probability of reaching the $s'$ state when the system takes the $a$ action from the $s$ state. To explain in more detail the elements that make up the state of the system by dividing a state $s$ into multiple states of $s_i$, the buffer state on link $i$ $b_i'$ depends on its own previous buffer state $b_i$ and its Ack state $k_i$, and whether HARQ is used on the previous action, which is $h$. Since an MCS state depends on the use of HARQ, and basically inherits the action of MCS, the MCS state $m_S'$ depends on $m_S'$, $k_i$, $h$, and $m_A$. The Ack can be determined by various factors. The Ack state for link $i$ $k_i'$ is dependent on the buffer state $b_i$, the former Ack state $k_i$, the channel state $c_i$, the HARQ action $h$, and the MCS action $m_A$. Meanwhile, since we are considering block fading channel model, the channel state on link $i$, $c_i'$, and the available slot state $f'$ depends on the available slot state $f$. To sum up, the state transition function for the link

$i$ can be expressed as follows:

$$\begin{aligned}\Pr\left[s_i'|s_i,a\right] = \Pr\left[b_i'|b_i,k_i,h\right] \\ \times \Pr\left[m_S'|m_S,k_i,h,m_A\right] \\ \times \Pr\left[k_i'|b_i,k_i,c_i,h,m_A\right] \\ \times \Pr\left[c_i'|c_i,f\right] \times \Pr\left[f'|f\right]. \end{aligned} \tag{11}$$

Therefore, we can define the state transition function concerning all links as follows:

$$\begin{aligned}\Pr\left[s'|s,a\right] = \prod_{i\in I}\Pr\left[b_i'|b_i,k_i,h\right] \\ \times \prod_{i\in I}\Pr\left[m_S'|m_S,k_i,h,m_A\right] \\ \times \prod_{i\in I}\Pr\left[k_i'|b_i,k_i,c_i,h,m_A\right] \\ \times \prod_{i\in I}\Pr\left[c_i'|c_i,f\right] \times \Pr\left[f'|f\right]. \end{aligned} \tag{12}$$

Looking at each element in (11) one by one, we can first derive the transition probability of $\mathbf{B}$ as follows. When HARQ is not applied, the buffer will always be flushed, according to the definition stated in III-C. Therefore, the transition probability from $b_i$ to $b_i'$ when $h = 0$ is defined as

$$\Pr\left[b_i'|b_i,k_i,h=0\right] = \delta\left(b_i,' 0\right), \tag{13}$$

where $\delta(x, y)$ is the Kronecker delta function. On the other hand, the receiver stacks up the current data frame for HARQ when 1) the previous transmission applied HARQ, and 2) the decoding of the transmission failed, unless the buffer has room for buffering the data frame. Therefore, the transition probability when $h = 1$ can be expressed as

$$\Pr\left[b_i'|b_i = B_{\max},k_i=0,h=1\right] = \delta\left(b_i,' b_i\right) \tag{14}$$

and

$$\Pr\left[b_i'|b_i \neq B_{\max},k_i=0,h=1\right] = \delta\left(b_i,' b_i+1\right). \tag{15}$$

The MCS depends on the use of HARQ, the MCS of the previous transmission, the transmission result of the previous transmission, and the transmitter's selected action. When HARQ is not used, the MCS has only to follow the action. Hence, the transmission probability of $\mathbf{M}_S$ when $h = 0$ can be explained as follows:

$$\Pr\left[m_S'|m_S,k_i,h=0,m_A\right] = \delta\left(m_S,' m_A\right). \tag{16}$$

As we assume that HARQ-CC is considered and the transmit duration is fixed, the MCS shall be the same as the previous transmission's MCS only if the transmission is a retransmission. Taken all together, the transmission probability of $\mathbf{M}_S$ when $h = 1$ can be explained as follows:

$$\begin{aligned}&\Pr\left[m_S'|m_S,k_i,h=1,m_A\right] \\ &= \begin{cases}\delta\left(m_S,' m_A\right) & \text{if } \ k_i=1, \\ \delta\left(m_S,' m_A\right)\cdot\delta\left(m_A,m_S\right) & \text{otherwise.}\end{cases}\end{aligned} \tag{17}$$

The Ack state stands for the results of the transmissions through the links. The Ack state $k'$ is represented by

$$\begin{aligned}&\Pr\left[k_i'|b_i,k_i,c_i,h,m_A\right] \\ &= \begin{cases}1-P_e\left(b_i,c_i,h,m_A\right) & \text{if } \ k_i'=1, \\ P_e\left(b_i,c_i,h,m_A\right) & \text{otherwise,}\end{cases}\end{aligned} \tag{18}$$

where $P_e(b_i, c_i, h, m_A)$ is the probability that a data packet transmitted will be received in error according to the amount of buffered data, the channel condition, the HARQ usage, and the MCS action. This probability can vary depending on the modulation and coding scheme used. Since HARQ-CC is known to ideally provide $\times 2$ of SNR gain from retransmission, for example, when using binary phase shift keying (BPSK), the data packet error probabilities according to the use of HARQ can be given by

$$P_e\left(b_i,c_i,h=0,m_A\right) = 1-\left(1-Q\left(\sqrt{\frac{2c_i}{N_0}}\right)\right)^{l(m_A)}, \tag{19}$$

and

$$P_e\left(b_i,c_i,h=1,m_A\right) = 1-\left(1-Q\left(\sqrt{\frac{2c_i}{N_0}\cdot 2b_i}\right)\right)^{l(m_A)} \tag{20}$$

where $Q(\cdot)$ represents the Gaussian tail function and $l(m_A)$ is the frame size of the data, depending on the selected modulation and coding scheme $m_A$, given the fixed data frame duration, $c_i$ is the channel state of link $i$, and $N_0$ is the noise power spectral density.

Under the block fading model, the channel is assumed to remain fixed unless the available slot remains. Thus, the channel states can be represented as

$$\Pr\left[c_i'|c_i,f\neq 0\right] = \delta\left(c_i,' c_i\right), \tag{21}$$

and

$$\Pr\left[c_i'|c_i,f=0\right] = \begin{cases}1/C_{\max}, & c_i,c_i' \in \mathbf{C}_i, \\ 0, & \text{otherwise.}\end{cases} \tag{22}$$

Finally, since the available slot is continuously decremented, the available slot states are defined as

$$\Pr\left[f'|f\neq 0\right] = \delta\left(f-1,f'\right), \tag{23}$$

and

$$\Pr\left[f'|f=0\right] = \delta\left(F_{\max}-1,f'\right). \tag{24}$$

### *E. Reward and Cost Functions*

We consider the normalized amount of delivered information and the normalized amount of buffer required for HARQ to define the reward and cost functions. First, the total reward function is defined as

$$R(s,a) = \alpha\cdot f(s,a) - (1-\alpha)\cdot g(s,a), \tag{25}$$

where $f(s, a)$ and $g(s, a)$ stands for the reward function and the cost function, given the state $s$ and the action $a$, respectively, Also $\alpha$ represents a weighted coefficient to prioritize between

expected throughput and buffer occupancy. Let another state in $\mathbf{S}_i$, which focuses on an individual link, as mentioned in (8) as $s_i = \{b_i, m_S, k_i, c_i, f\}$, then the total reward function in (25) can be rewritten as

$$R(s,a) = \sum_{i \in I} (\alpha \cdot f(s_i, a) - (1-\alpha) \cdot g(s_i, a)). \tag{26}$$

Given the current state $s_i$ for link $i$ and the decided action $a$, the reward function is defined as

$$f(s_i, a) = \sum_{s_i' \in \mathbf{S}_i} \Pr[s_i' | s_i, a] \cdot \hat{f}(s_i' | s_i, a). \tag{27}$$

As we set up the reward function with the normalized amount of delivered information, the reward function for link $i$ is as follows:

$$\hat{f}(s_i' | s_i, a) = \begin{cases} l(m_A)/l(M), & \text{if } k_i' = 1, \\ 0, & \text{otherwise.} \end{cases} \tag{28}$$

For example, let $M_L$ and $M_H$ be low MCS and high MCS, respectively, $l(M_L)$ is smaller than $l(M_L)$ since we are assuming fixed frame duration. It is clear that the buffer needs to be flushed after successful decoding. Hence, considering only the valid states, the reward function for link $i$ is as follows:

$$f(s_i, a) = (1 - P_e(s_i, a)) \cdot \frac{l(m_A)}{l(M)}, \tag{29}$$

with corresponding conditions described in (13)–(24), where $P_e(b_i, c_i, h, m_A)$, which is represented in (18), is expressed in more simple way as $P_e(s_i, a)$, and $l(m_A)$ is as defined in (19) and (20).

Meanwhile, the cost function for link $i$ describing the normalized buffer occupancy is defined as

$$g(s_i, a) = \sum_{s_i' \in \mathbf{S}_i} \Pr[s_i' | s_i, a] \cdot \hat{g}(s_i' | s_i, a), \tag{30}$$

where

$$\hat{g}(s_i' | s_i, a) = \begin{cases} 1/B_{\max}, & \text{if } b_i \neq B_{\max}, k_i' = 0, h = 1, \\ 0, & \text{if } b_i = B_{\max}, k_i' = 0, h = 1, \\ -b_i/B_{\max}, & \text{otherwise.} \end{cases} \tag{31}$$

In a similar way to the reward function in (27)–(29), the cost function can be described as

$$g(s_i, a) = \left(1 - P_e(s_i, a|_{h=1})^{B_{\max}+1}\right) \cdot \frac{1}{B_{\max}} - (1 - P_e(s_i, a|_{h=1})) \cdot \frac{b_i}{B_{\max}} \tag{32}$$

with the same conditions considered in (13)–(24). Then, the total reward $R(s,a)$ can be computed with (25)–(29).

### F. Objective Function and Operation Example

HARQ-based retransmission control policy $\pi$ describes decision rules that determine the action taken by the transmitter. It maps the current state space to the action space to take in the current decision epoch. The goal here is to find a policy that maximizes the total reward $R(s,a)$, which is expressed in (25), expected by the transmitter over an infinite time horizon, which is given by

$$V_\pi(s_0) = \lim_{t \to \infty} \frac{1}{t} E_\pi \left[ \sum_{n=1}^{t} R(S_n, a_n) | S_0 = s_0 \right], \tag{33}$$

where $n$ is the index of the time epoch, $S_n$ and $a_n$ are the state space and the action space on the time epoch $n$, respectively, $s_0$ is the initial state, and $E_\pi$ is the expected reward with the policy $\pi$.

Since we are aiming at maximizing the expected total reward, the optimal equation, which is well known as the Bellman optimality equation [35], can be represented as

$$V_*(s_0) = \max_{a \in A} \left\{ r(s_0, a) + \sum_{s' \in S} \lambda \Pr[s' | s_0, a] V_*(s') \right\}, \tag{34}$$

where $\lambda$ is a discount factor for the MDP model and $r(s_0, a)$ is an initial reward when the agent, which is the MLD in this article, on the initial state $s_0$ decides to select action $a$. There are several algorithms that solve the optimization problem, including value iteration, policy iteration, and prioritized sweeping [36]. To solve the optimal equation and obtain the optimal policy for each state $\pi^*(s)$, we decide to use the value iteration algorithm as shown in Algorithm 1.

**Algorithm 1:** Value Iteration Algorithm for HARE.

1: Set $V_0(s) = 0$ for each state $s$. Specify $\epsilon$ and set $k = 0$.
2: Define the value function $V_k(s)$ as

$$V_k(s) = \max_{a \in A} \{ r(s,a) + \sum_{s' \in S} \lambda \Pr[s' | s, a] V_{k-1}(s') \}.$$

3: For each state $s \in \mathbf{S}$, compute $V_1(s)$.
4: **while** $\|V_{k+1} - V_k\| \geq \epsilon(1-\lambda)/2\lambda$ **do**
5: Increase $k$ by 1.
6: For each state $s \in \mathbf{S}$, compute $V_{k+1}(s)$.
7: For each state $s$, compute the stationary optimal policy

$$\pi^*(s) = \arg\max_{a \in A} \{ r(s,a) + \sum_{s' \in S} \lambda \Pr[s' | s, a] V_{k-1}(s') \}$$

8: **return** $\pi^*(s)$.

In this algorithm, the norm function $\|V_k\|$ is defined by $\|V_k\| = \max |V_k(s)|$ for $s \in \mathbf{S}$. As seen in the algorithm, it performs within $O(|A||S|^2)$ for each iteration. To reduce the computational complexity, a table can be used to store the optimal policy, which can be computed in advance by the value iteration algorithm. In doing so, each device only computes the algorithm only once. Hence, this HARE algorithm can be scalable even when lots of non-AP MLDs are attached to a single AP MLD.

To ease your understanding, we elaborate on the detailed timeline following HARE operation as shown in Fig. 4. As seen at the time epochs of $T_1$ and $T_3$, the actions of MCS selection are always identical to their former MCS indices unless all the

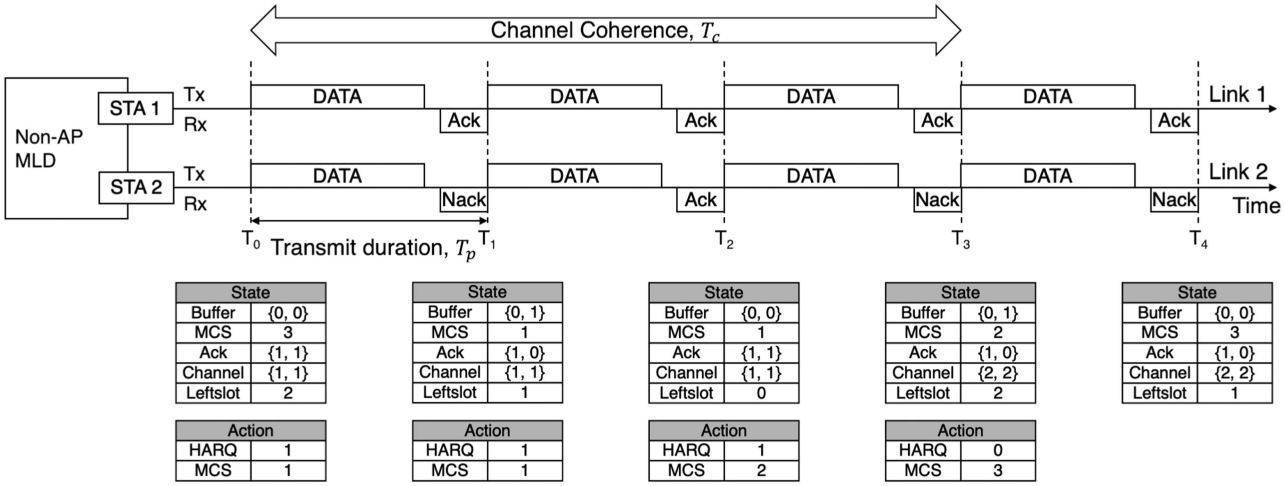


Fig. 4. An illustrative example of state information and its corresponding decisions on decision epochs for HARE.

transmissions are successfully received when HARQ is used. On the other hand, as can be seen from the point of $T_2$, all transmissions are confirmed by the Ack frame, so the transmitter can change the MCS index even if it wishes to use HARQ. Assuming that the channel coherence time has ended and the transmitter has detected that the channel is in good condition, as seen at $T_3$, the transmitter can consider choosing a high MCS index while giving up buffered frames rather than choosing the lower MCS index previously selected for HARQ.

## IV. Performance Analysis Results

For performance analysis, we conducted extensive simulations with MATLAB R2020a and compared the proposed algorithm, HARE, with the ARQ-only algorithm and the HARQ-only algorithm. The ARQ-only algorithm does not apply HARQ, and thus it does not require any buffer space. Also, the ARQ-only algorithm is a conventional retransmission policy in IEEE 802.11 so far. On the other hand, The HARQ-only algorithm always applies HARQ. Hence, the MCS would be fixed unless the corresponding transmission is successfully received. Both ARQ-only and HARQ-only also conduct the same MDP modeling process, presented in Section II.

In this analysis, we assume that the PHY preambles in all frames are decoded without fail. We also consider that two stations are attached to one non-AP MLD, each of which forms a link to each AP affiliated with the same AP MLD. We used the value of the discount factor $\lambda = 0.95$. Used parameters are enumerated in Table II, and other parameters that are not mentioned follow the IEEE 802.11be draft standard of version 2.3, which is the latest standard amendment for WLAN. Specifically, transmit duration was referred to aPPDUMaxTime of EHT PHY characteristics of IEEE 802.11be, and supportable data rates are EHT-MCS index of 0, 1, 2, and 3 for 242-tone resource unit (RU), which means 20 MHz channel, with the number of spatial streams are one. In detail, the supportable data rates are defined as BPSK with 1/2 forward error correction (FEC) coding rate, quadrature phase-shift keying (QPSK) with 1/2 FEC coding rate, QPSK with 3/4 FEC coding rate, and 16-QAM with 1/2 FEC coding rate, respectively. We use the listed parameters unless we are observing the effect of the specific parameter.

TABLE II
Summary of Simulation Parameters

| Parameter | Value |
|---|---|
| Number of links, $\|I\|$ | 2 |
| Average signal-to-noise ratio | 10 dB |
| Transmit duration, $T_p$ | 5.484 $\mu$s |
| Guard interval | 1.6 $\mu$s |
| Supportable data rates (Mbps) | 8.1, 16.3, 24.4, 32.5 |
| Mobility speed, $v$ | 1.4 m/s |
| Channel model | Rayleigh block fading |
| Noise spectral density, $N_0$ | 1 |
| Discount factor for value iteration, $\lambda$ | 0.95 |
| Weighted coefficient, $\alpha$ | 0.95 |
| Number of buffers per one frame, $B_{\max}$ | 2 |
| Maximum retransmission count for HARQ | 2 |
| Number of MCS states, $M$ | 4 |
| Number of discretized channel states, $C_{\max}$ | 2 |

### A. Effect of Weighted Coefficient

As defined in (25), $\alpha$ is a weighted coefficient to prioritize between throughput and buffer occupancy. Fig. 5 shows expected throughput and normalized buffer occupancy for each algorithm, respectively. In Fig. 5(a), we can see that the expected throughput of HARE exceeds those of the ARQ-only and HARQ-only algorithms by 15.6% and 95%, when $\alpha = 1$, respectively. As large $\alpha$ describes that we prioritize increasing the throughput, rather than decreasing the buffer amount, we can see that the throughputs of HARE gradually increase as $\alpha$ increases. Since the ARQ-only algorithm does not use buffer, we can see that its throughput remains equal, except $\alpha = 0$. On the other hand, the HARQ-only algorithm will try to take relatively higher MCS as $\alpha$ increases. However, since MCS gets fixed during retransmissions when HARQ is applied, this overestimated reward leads to lots of retransmissions and causes poor performance for higher $\alpha$.

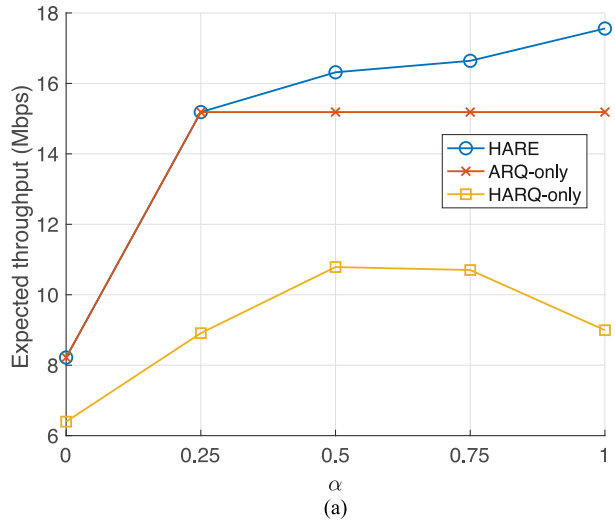


Fig. 5. Effect of $\alpha$. (a) The expected throughputs. (b) The normalized buffer occupancies.

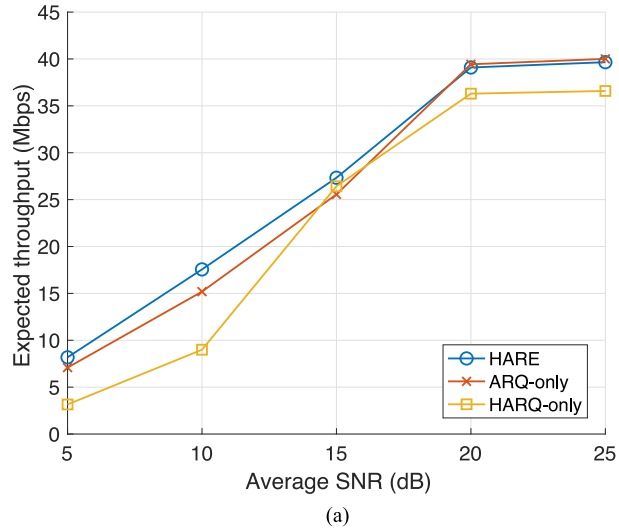


Fig. 6. Effect of average SNR. (a) The expected throughputs. (b) The normalized buffer occupancies.

The normalized buffer occupancy is shown in Fig. 5(b). Normalized amount of buffered data, expressed in y-axis, stands for the ratio of occupancy rate per one delivered packet. Contrary to the former case, smaller $\alpha$ aims at reducing occupied buffer size. We can observe that the amount of buffered data for HARE is from 50% to 97% smaller than that of HARQ-only algorithm. Since the ARQ-only algorithm does not use any buffer for HARQ combining, it is obvious that the ARQ-only algorithm's buffer occupancy remains zero for all the time. We can see that the buffer occupancy for the HARQ-only algorithm tends to reduce as $\alpha$ decreases, but the variation is insignificant. However, HARE can significantly reduce the amount of buffered data, which can be done by applying HARQ adaptively. With the weighted value $\alpha$, HARE can adaptively prioritize the throughput to the occupied buffer size. In conclusion, we can observe that HARE can outperform the conventional ARQ-only and HARQ-only algorithms with the help of reasonable buffer space and adaptive use of HARQ.

### B. *Effect of Average SNR*

Fig. 6(a) and (b) show the effect of the average SNR. When it comes to the expected throughputs, illustrated in Fig. 6(a), the HARQ-only algorithm is relatively inferior to the other algorithms when the average SNR is relatively low or high. Since the low SNR leads to lots of retransmissions, the HARQ-only algorithm takes up much buffer space. Furthermore, in high average SNR situation, since only a few transmissions fail, HARQ will be unnecessary. On the other hand, when a transmitter in HARE determines that the use of HARQ is useless because the channel condition is too bad, the transmitter does not attempt to use HARQ. When the average SNR is high, most of the initial transmissions will successfully be decoded without any retransmission, which is the reason why all the algorithms' throughputs become nearly equal for high SNR.

For the buffer occupancy, shown in Fig. 6(b), since it is widely known that HARQ is effective when channel conditions are poor, the buffer occupancy decreases as the SNR increases.

TABLE III
THROUGHPUTS AND AVERAGE BUFFER SIZES ACCORDING TO MOBILITY SPEED

| Mobility speeds | | 5 m/s | 3 m/s | 2 m/s | 1.4 m/s |
|---|---|---|---|---|---|
| Coherence slots | | 1 | 2 | 3 | 4 |
| HARE | Throughputs (Mbps) | 17.603 | 17.383 | 16.949 | 16.383 |
| | Average buffer occupancy | 6.7% | 4.5% | 1.9% | 0.2% |
| ARQ-only | Throughputs (Mbps) | 17.143 | 16.737 | 16.700 | 16.383 |
| | Average buffer occupancy | 0% | 0% | 0% | 0% |
| HARQ-only | Throughputs (Mbps) | 12.020 | 12.292 | 12.861 | 15.085 |
| | Average buffer occupancy | 31.6% | 31.1% | 30.3% | 26.9% |

Overall, the throughput of HARE outperforms the other algorithms in terms of the expected throughput with various channel conditions.

### C. Effect of Mobility Speed

Table III shows the effect of throughputs and the average buffer sizes when the mobility speed varies. In order to take a look at variations of throughputs and average buffer sizes of HARE, ARQ-only, and HARQ-only algorithms deliberately, we set $\alpha$ to 0.5.

As mentioned in Section III-A, the speed of mobility is related to the maximum Doppler shift. When the mobility of devices is high, the instantaneous SNR fluctuates, and thus channel coherence time $T_c$ becomes short.

Since ARQ-only algorithm does not use buffer, its average buffer occupancy ratio is obviously zero. Also, we can find that the throughput for ARQ-only algorithm slightly decreases as the mobility speed becomes high.

Let us take a look at the case of HARQ-only algorithm. In general, buffered packets for HARQ constantly occupy device's buffer. It is worth noting that the lower the mobility, the longer the consistency of the channel, so the retransmitted packet is likely to be recovered using the buffered packet. This can be confirmed through throughputs of HARQ-only algorithm. On the other hand, when mobility is high, the channel consistency dynamically changes. For HARQ-only algorithm, the same MCS as the previous transmission should be used for retransmissions for HARQ combining, which may not be suitable for dynamic channel environments, resulting in poor performance compared to others even though failed packets are buffered.

In the case of HARE, it can be seen that the higher the mobility, the lower the average buffer occupancy. In addition, it can be observed that the overall throughput of HARE is similar to or higher than that of the ARQ-only algorithm with small buffer for HARQ combining operation.

### D. Analysis of Optimal Policy Affected by the Number of Available Slots

Fig. 7 shows the probability mass functions that give the probability of selecting each action in the available slot by the channel coherence. In these figures, $f$ stands for the number of available slots by the channel coherence. The device is supposed to apply HARQ if $h = 1$, with MCS of $m_A$. Otherwise, the device will not apply HARQ if $h = 0$. In this subsection, we will observe how the transmitter behaves in each algorithm.

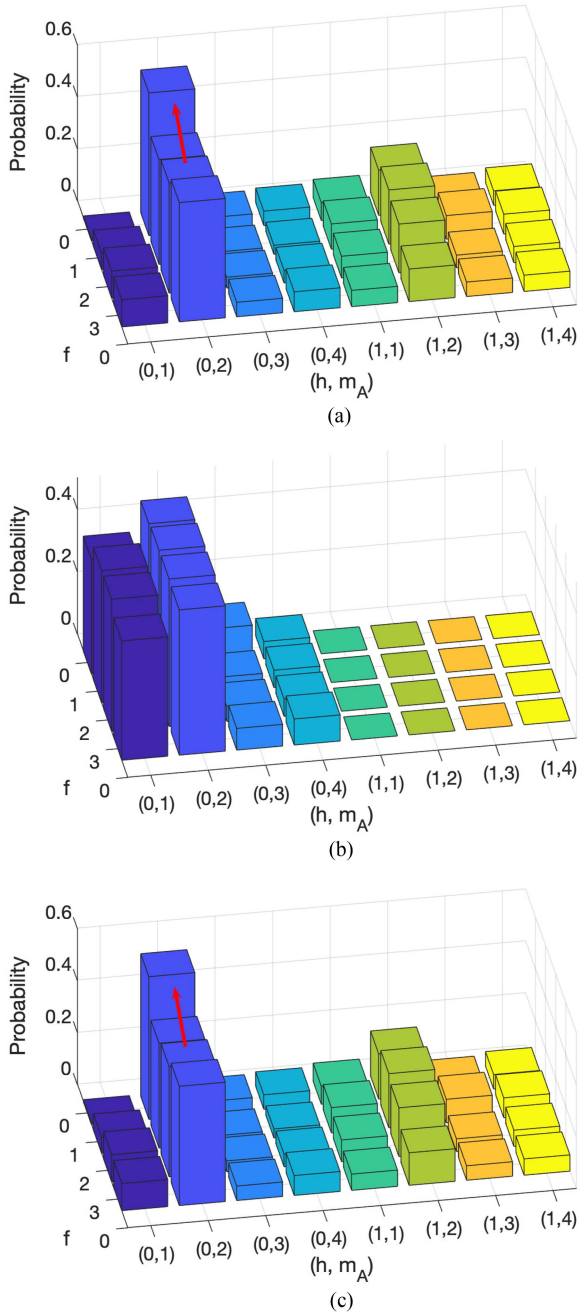


Fig. 7. Optimal policies for HARE, ARQ-only, and HARQ-only algorithms. (a) HARE. (b) ARQ-only algorithm. (c) HARQ-only algorithm.

As stated in Table II, the average SNR is set to 10 dB. In this nearby SNR area, selecting MCS 2 is most appropriate. Thus, all the algorithms are likely to select $m_A = 2$. Fig. 7(a) shows the probability mass function for HARE. The most significant part is that as $f$ becomes zero, indicated by the red arrow, especially where $f = 0$ and $(h, m_A) = (0, 2)$, HARE is likely not to apply HARQ. In a practical situation, the device will check the channel

condition once every few milliseconds. This observation shows us that if a long time has passed since measuring the channel status, it is better to use the conventional ARQ transmission after flushing out the buffer.

In Fig. 7(b), we can see that the ARQ-only algorithm determines transmission's MCS index in a conservative manner. The reason for it is that the ARQ-only algorithm cannot utilize the buffered data, and thus, it cannot take advantage of them. On the other hand, as shown in Fig. 7(c), the HARQ-only algorithm tends to select the MCS more aggressively.

## V. Conclusion

In this article, we proposed HARE, a retransmission algorithm that adaptively applies HARQ and selects an appropriate MCS while requiring relatively low buffer occupancy in a multi-link WLAN, where HARQ-CC and synchronous multi-link transmission are considered. To find out the optimal policy to maximize the reward consisting of the expected throughput and the buffer occupancy, we formulated a Markov decision process that considers the current buffer status, the channel condition, the result of the previous transmission, and the channel coherence time. Performance analysis demonstrated that HARE could perform higher throughput compared to ARQ-only and HARQ-only algorithms. Also, it was shown that HARE requires a lower buffer amount than the algorithm using HARQ. We will investigate how to apply HARE when the transmissions need not be aligned in our future work.

## References


[1] Cisco, "Cisco Annual Internet Report (2018–2023)," 2020. [Online]. Available: https://www.cisco.com/c/en/us/solutions/collateral/executive-perspectives/annual-internet-report/white-paper-c11-741490.html

[2] A. Feldmann et al., "The lockdown effect: Implications of the COVID-19 pandemic on internet traffic," in *Proc. ACM Internet Meas. Conf.*, ser. IMC '20, 2020, pp. 1–18, doi: 10.1145/3419394.3423658.

[3] IEEE, "IEEE P802.11 - TASK GROUP BE (EHT) - GROUP INFORMATION UPDATE," 2023. [Online]. Available: http://www.ieee802.org/11/Reports/tgbe_update.htm

[4] R. Comroe and D. Costello, "ARQ schemes for data transmission in mobile radio systems," *IEEE J. Sel. Areas Commun.*, vol. 2, no. 4, pp. 472–481, Jul. 1984.

[5] P. Frenger, S. Parkvall, and E. Dahlman, "Performance comparison of HARQ with chase combining and incremental redundancy for HS-DPA," in *Proc. IEEE Veh. Technol. Conf.*, 2001, vol. 3, no. 54ND, pp. 1829–1833.

[6] K. C. Beh, A. Doufexi, and S. Armour, "Performance evaluation of hybrid ARQ schemes of 3GPP LTE OFDMA system," in *Proc. IEEE 18th Int. Symp. Personal, Indoor Mobile Radio Commun.*, 2007, pp. 1–5.

[7] E. Cabrera, G. Fang, and R. Vesilo, "Adaptive hybrid ARQ (A-HARQ) for ultra-reliable communication in 5G," in *Proc. IEEE 85th Veh. Technol. Conf.*, 2017, pp. 1–6.

[8] S. Shilo, L. Epstein, Y. Ben Arie, and E. Melzer, "HARQ for EHT," 2018. [Online]. Available: https://mentor.ieee.org/802.11/dcn/18/11-18-1587-01-0eht-harq-for-eht.pptx

[9] Y. Zhang, H. Zhang, S. Srinivasa, L. Chu, R. Cao, and M. Yu, "HARQ Feasibility," 2019. [Online]. Available: https://mentor.ieee.org/802.11/dcn/18/11-18-1992-01-0eht-harq-feasibility.pptx

[10] Y. Zhang, H. Zhang, S. Srinivasa, L. Chu, R. Cao, and M. Yu, "Comparisons of HARQ transmission schemes for 11be," 2019. [Online]. Available: https://mentor.ieee.org/802.11/dcn/19/11-19-0792-02-00be-comparisons-of-harq-transmission-schemes-for-11be.pptx

[11] Y. Ding, L. Huang, R. Chitrakar, and Y. Urabe, "HARQ punctured CC performance evaluation," 2019. [Online]. Available: https://mentor.ieee.org/802.11/dcn/19/11-19-1146-00-00be-harq-punctured-cc-performance-evaluation.pptx

[12] S. Shellhammer, Z. Doan, A. Chen, and B. Tian, "HARQ simulation results," 2019. [Online]. Available: https://mentor.ieee.org/802.11/dcn/19/11-19-1078-00-00be-harq-simulation-results.pptx

[13] K. Oteri, L. H. Sun, R. Yang, X. Wang, J. Levy, and A. Sahin, "Hybrid ARQ in collision free and collision dominated environments," 2019. [Online]. Available: https://mentor.ieee.org/802.11/dcn/19/11-19-0070-00-0eht-hybrid-arq-in-collision-free-and-collision-dominated-environments.pptx

[14] K. Oteri, L. H. Sun, R. Yang, X. Wang, J. Levy, and A. Sahin, "Effect of preamble decoding on HARQ in 802.11be," 2019. [Online]. Available: https://mentor.ieee.org/802.11/dcn/19/11-19-0390-00-0eht-effect-of-preamble-decoding-on-harq-in-802-11be.pptx

[15] J. Kim, T. Song, E. Park, D. Lim, and J. Choi, "Channel coding issue in HARQ," 2019. [Online]. Available: https://mentor.ieee.org/802.11/dcn/19/11-19-1132-02-00be-channel-coding-issue-in-harq.pptx

[16] I. Jang, J. Choi, J. Kim, S. Kim, S. Park, and T. Song, "Channel access for multi-link operation," 2019. [Online]. Available: https://mentor.ieee.org/802.11/dcn/19/11-19-1144-06-00be-channel-access-for-multi-link-operation.pptx

[17] S. Hwang, J. Oh, K. Kang, Y. Gwak, H. Hong, and R. Y. Kim, "Consideration on multi-link operation," 2019. [Online]. Available: https://mentor.ieee.org/802.11/dcn/19/11-19-1181-01-00be-consideration-on-multi-link-operation.pptx

[18] S. Naribole, S. Kandala, W. B. Lee, and A. Ranganath, "Multi-link TXOP aggregation considerations," 2019. [Online]. Available: https://mentor.ieee.org/802.11/dcn/19/11-19-1505-02-00be-multi-link-aggregation-considerations.pptx

[19] Y. Li, Y. Li, Y. Guo, M. Gan, G. Huang, and Y. Zhou, "Discussion about single and multiple primary links in synchronous multi-link," 2019. [Online]. Available: https://mentor.ieee.org/802.11/dcn/19/11-19-1993-01-00be-discussion-about-single-and-multiple-primary-channels-in-synchronous-multi-link.pptx

[20] D. Ho, A. Patil, G. Cherian, and A. Asterjadhi, "MLA: Sync PPDUs," 2020. [Online]. Available: https://mentor.ieee.org/802.11/dcn/20/11-20-0026-07-00be-mlo-sync-ppdus.pptx

[21] Z. Lan, A. Bredewoud, G. Kondylis, and M. Fischer, "MLO a-synchronize and synchronize operation discussions," 2020. [Online]. Available: https://mentor.ieee.org/802.11/dcn/20/11-20-0291-01-00be-mlo-async-and-sync-operation-discussion.pptx

[22] L. Chu et al., "Multiple link operation follow up," 2020. [Online]. Available: https://mentor.ieee.org/802.11/dcn/20/11-20-0487-05-00be-multiple-link-operation-follow-up.pptx

[23] T. Song and T. Kim, "Performance analysis of synchronous multi-radio multi-link MAC protocols in IEEE 802.11be extremely high throughput WLANs," *Appl. Sci.*, vol. 11, no. 1, 2021, Art. no. 317.

[24] Á. López-Raventós and B. Bellalta, "IEEE 802.11be multi-link operation: When the best could be to use only a single interface," 2021. [Online]. Available: http://arxiv.org/abs/2105.10199

[25] S. Naribole, W. B. Lee, S. Kandala, and A. Ranganath, "Simultaneous transmit-receive multi-channel operation in next generation WLANs," in *Proc. IEEE Wireless Commun. Netw. Conf.*, 2020, pp. 1–8.

[26] S. Naribole, S. Kandala, and A. Ranganath, "Multi-channel mobile access point in next-generation IEEE 802.11be WLANs," in *Proc.-IEEE Int. Conf. Commun.*, 2021, pp. 1–7.

[27] A. López-Raventós and B. Bellalta, "Multi-link operation in IEEE 802.11be WLANs," *IEEE Wireless Commun.*, vol. 29, no. 4, pp. 94–100, Aug. 2022.

[28] B. Medepally, N. B. Mehta, and C. R. Murthy, "Implications of energy profile and storage on energy harvesting sensor link performance," in *Proc. IEEE Glob. Telecommun. Conf.*, 2009, pp. 1–6.

[29] A. Aprem, C. R. Murthy, and N. B. Mehta, "Transmit power control policies for energy harvesting sensors with retransmissions," *IEEE J. Sel. Topics Signal Process.*, vol. 7, no. 5, pp. 895–906, Oct. 2013.

[30] P. Wu and N. Jindal, "Performance of Hybrid-ARQ in block-fading channels: A fixed outage probability analysis," *IEEE Trans. Commun.*, vol. 58, no. 4, pp. 1129–1141, Apr. 2010.

[31] T. S. Rappaport et al., *Wireless Communications: Principles and Practice*, vol. 2. Englewood Cliffs, NJ, USA: Prentice Hall, 1996.

[32] E. N. Gilbert, "Capacity of a burst-noise channel," *Bell Syst. Tech. J.*, vol. 39, no. 5, pp. 1253–1265, 1960.

[33] E. O. Elliott, "Estimates of error rates for codes on burst-noise channels," *Bell Syst. Tech. J.*, vol. 42, no. 5, pp. 1977–1997, 1963.
[34] Q. Zhang and S. A. Kassam, "Finite-state Markov model for rayleigh fading channels," *IEEE Trans. Commun.*, vol. 47, no. 11, pp. 1688–1692, Nov. 1999.
[35] D. P. Bertsekas, *Dynamic Programming and Optimal Control*, vol. 1. Belmont, CA, USA: Athena Scientific, 1995 .
[36] M. L. Puterman, *Markov Decision Processes: Discrete Stochastic Dynamic Programming*. Hoboken, NJ, USA: Wiley, 2014.

**Taewon Song** received the B.S. and Ph.D. degrees in electrical engineering from Korea University, Seoul, South Korea, in 2010 and 2017, respectively. In 2021, he joined Soonchunhyang University, Asan, South Korea, where he is currently an Assistant Professor with the SCH Convergence Science Institute. From 2017 to 2020, he was a Senior Researcher with the Advanced Standard R&D Laboratory, LG Electronics, where he worked on standardization for wake-up radio and next-generation WLANs. From February 2015 to April 2015, he was a Visiting Student supported by the BK21+ project with the University of Florida, Gainesville, FL, USA. From January 2012 to February 2012, he was a Visiting Researcher supported by the National Research Foundation of Korea, National Institute of Information and Communications Technology. His research interests include AI-empowered networking, low-power wake-up radio, and the wireless medium access control protocol of next-generation WLANs.

**Woong-Hee Lee** received the B.S. degree in electrical engineering from the Korea Advanced Institute of Science and Technology, Daejeon, South Korea, in 2009, and the Ph.D. degree in electrical engineering from Seoul National University, Seoul, South Korea, in 2017. In 2009, he entered the combined Master's and Doctoral Program. From 2017 to 2019, he was an Experienced Researcher with the Advanced Standard Research and Development Laboratories, LG Electronics Inc., Seoul, South Korea. From 2019 to 2020, he was a Postdoctoral Researcher with the Department of Communication Systems, KTH Royal Institute of Technology, Stockholm, Sweden. From 2019 to 2020, he was an Experienced Researcher with Ericsson Research, Stockholm, Sweden. Since March 2021, he has been an Assistant Professor with the Department of Control and Instrumentation Engineering, Korea University, Sejong-si, South Korea. His research interests include signal processing, machine learning, and game theory in wireless communications.